

Hydratable Channels: Structural and Fluorescent Probes of Position and Function in a Phospholipid Bilayer

Ernesto Abel, Glenn E. M. Maguire, Oscar Murillo, Iwao Suzuki, Stephen L. De Wall, and George W. Gokel^{*,†}

Contribution from the Bioorganic Chemistry Program and Department of Molecular Biology & Pharmacology, Washington University School of Medicine, 660 South Euclid Avenue, Campus Box 8103, St. Louis, Missouri 63110

Received March 22, 1999

Abstract: Three novel tris(macrocycle)s having fluorescent residues at their distal termini have been prepared and studied. The compounds are of the form R(N18N)C₁₂(N18N)C₁₂(N18N)R in which R is 2-(3-indolyl)-ethyl (**1**), 2-(3-(*N*-methylindolyl))ethyl (**2**), and dansyl (**3**). Compounds **2** and **3** were found to transport Na⁺ at rates similar to those of other tris(macrocycle)s but **1** was not an ionophore in the bilayer as assessed by ²³Na NMR analysis. The latter failure may be due to a hydrogen-bond blockade leading to a globular conformation adopted by the hydratable. The fluorescence maximum of **3** was determined in a variety of solvents and in a phospholipid bilayer. The polarity experienced by the dansyl group in the bilayer was intermediate between that observed in methanol and ethanol. Fluorescence depth quenching using doxyl-substituted lipids showed that the dansyl headgroups of **3** were 14 Å from the bilayer's midplane or separated by about 28 Å. Fluorescence energy transfer between **2** and **3** showed that these two hydratables were not appreciably aggregated in the bilayer.

Introduction

Proteins that span phospholipid membranes and mediate the transport of cations, anions, and molecules across the boundaries of cells and organelles are crucial to all life. This fact has made the study of transmembrane ion channels one of the most active areas in modern biological chemistry.^{1,2} The fundamental importance of this area in general and of the mechanistic questions concerning channel function in particular cannot be overstated. An enormous amount of information has accumulated on which proteins are responsible for transport but the physical and chemical details of transport and selectivity remain largely obscure.³ During the past year, important solid-state structural results for the *KscA* K⁺ channel⁴ of *Streptomyces lividans* and the mechanosensitive channel⁵ of *Mycobacterium tuberculosis* have clarified structural relationships in natural protein channels.

An alternative to the study of channel-forming peptides⁶ and proteins is the use of synthetic organic chemical model systems. Several synthetic compounds have been prepared that were designed either to function as channels or whose structures

appeared to be "channel-like". The principal of "property design"⁷ has been applied in the development of synthetic channel model systems by us⁸ and by others.⁹ Our own cation channel model system involves several features. Crown ethers were incorporated to function both as headgroups in the amphiphilic sense and as cation entry portals. The headgroups are connected via a hydrophobic spacer to a "relay" unit that is midway between the two.¹⁰ The latter two elements are apparent in the structure of the *Streptomyces lividans KscA* channel.⁴ Initially, all of the structures prepared were tris(macrocycle)s. As our designs became more elaborate, we dubbed the structures "hydratables." This name, which derives from the mythical, two-headed beast slain by Hercules, is evocative of the chemical function.

We have speculated that certain amino acids may function in transmembrane proteins to stabilize the helix positions with respect to each other and to the bilayer.¹¹ A candidate for this stabilization was indole, the side chain of the least prevalent of the common amino acids—tryptophan. Cross and co-workers showed by oriented NMR experiments that the multiple tryptophan residues of the channel-forming peptide gramicidin are directed toward the aqueous/bilayer interface.¹² We demonstrated experimentally that *N*-alkylindoles could form stable vesicles though the headgroups are neutral, the alkyl chain is attached at the H-bonding nitrogen atom, and only a single alkyl chain is present in the amphiphile.¹¹ The indolyl residue thus presented us with a useful, biologically relevant, and fluorescent probe for further studies into headgroup position in these hydratables.

The goals of the present work were to establish, so far as possible at this stage, (1) the location of the hydratable channels within the bilayer of the distal macrocycles, (2) the aggregation

[†] Tel: 314/362–9297. FAX: 314/362–9298 or 7058. E-mail: ggokel@moledool.wustl.edu.

(1) Nicholls, D. G. *Proteins, Transmitters, and Synapses*; Blackwell Science: Oxford, 1994.

(2) (a) Henderson, R.; Baldwin, J. M.; Ceska, T. A.; Zemlin, F.; Beckmann, E.; Downing, K. H. *J. Mol. Biol.* **1990**, *213*, 899–929. (b) Deisenhofer, J.; Epp, O.; Miki, K.; Huber, R.; Michel, H. *Nature* **1985**, *318*, 618–624. (c) Baldwin, J. M. *EMBO J.* **1993**, *12*, 1693–1703.

(3) (a) Stein, W. D. *Channels, Carriers, and Pumps*; Academic Press: New York, 1990. (b) Hille, B. *Ionic Channels of Excitable Membranes*; Sinauer Press: Sunderland, MA, 1992.

(4) Doyle, D. A.; Cabral, J. M.; Pfuetzner, R. A.; Kuo, A.; Gulbis, J. M.; Cohen, S. L.; Chait, B. T.; MacKinnon, R. *Science* **1998**, *280*, 69–77.

(5) Chang, G.; Spencer, R. H.; Lee, A. T.; Barclay, M. T.; Rees, D. C. *Science* **1998**, *282*, 2220–2226.

(6) Åkerfeldt, K. S.; Lear, J. D.; Wasserman, Z. R.; Chung, L. A.; DeGrado, W. F. *Acc. Chem. Res.* **1993**, *26*, 191–197. (b) Bechinger, B. J. *Membr. Biol.* **1997**, *156*, 197–211.

(7) Gokel, G. W.; Medina, J. C.; Li, C. *Synlett* **1991**, 677–683.

(8) Murillo, O.; Watanabe, S.; Nakano, A.; Gokel, G. W. *J. Am. Chem. Soc.* **1995**, *117*, 7665–7679.

state of the channel molecules, and (3) whether indole can play a headgroup stabilizing effect such as tryptophan apparently does in gramicidin. We report here the results of studies intended to answer these questions.

Results and Discussion

Design of Cation Channels. The compounds that are the subject of the studies described here are all tris(macrocyclic)s. They were designed to be flexible and structurally adaptive, as were the related carrier molecules that we designated "lariat ethers".¹³ It was intended in the original design that the central macrocycle would be parallel to the distal rings and would serve as a central "relay" through which cations would pass in transit. On the basis of previous and emerging evidence,¹⁴ we postulate that the central macrocycle adopts a conformation such that it is aligned with the bilayer's lipid chains. Such a conformation would diminish the local polarity of the macrocycle at the midplane of the bilayer and also afford interaction points for water and/or cations⁴ over a greater linear distance. Our current working model for the channel structure is shown in Figure 1. Note that intrachannel water, which we are confident is present, is shown but there is currently no evidence that the system enjoys the high level of order illustrated. It is likely that water

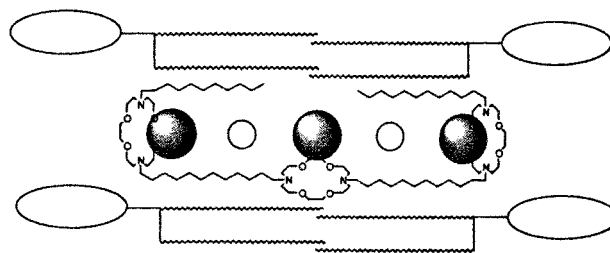
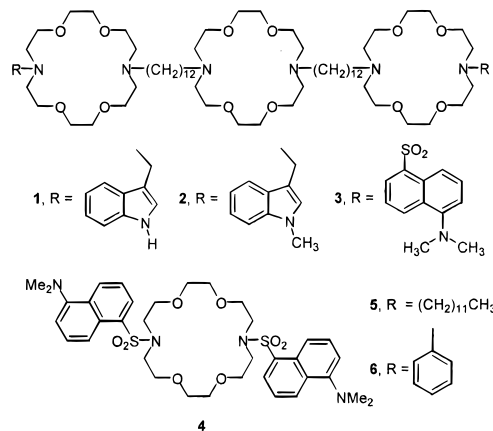


Figure 1. Schematic illustration of the presumed position of hydrophilic 7 within the phospholipid bilayer membrane.

fills spaces within the pore while being associated with (partially hydrating) cations. It should also be noted that the illustration shows the headgroup regime of a phospholipid approximately in proportion to the lipid chain length (although the headgroups may be canted rather than extended¹⁵). The tris(macrocyclic) channels were designed to span the insulator regime ("hydrocarbon slab"), a distance of 30–35 Å.

Compounds Required for the Studies. Two residues were chosen because they have well-documented fluorescent properties: indolyl (**1**) and dansyl¹⁶ (**3**). In addition to being fluorescent,¹⁷ indolyl has been postulated to serve as a membrane-anchoring residue in proteins.¹⁸ The ability of the indolyl N-H to serve as a hydrogen bond donor was potentially troublesome (see below) in conformational terms so the N-methylated analogue, **2**, was also prepared.

Compounds prepared for use in the present study are tris(macrocyclic)s of the general form R(N18N)C₁₂(N18N)C₁₂(N18N)R.¹⁹ We refer to the dodecyl chains as "spacers" and to the pendant "R" groups as headgroup chains. Tris(macrocyclic)s **1** and **2** have 2-(3-indolyl)ethyl and 2-(N-methyl-3-indolyl)ethyl headgroup chains, respectively. The (3-indolyl)methyl group is



the side chain present in tryptophan. Compound **3** is terminated by the dimethylaminosulfonyl (dansyl, Dn) groups. The diaza-

(15) Hauser, H.; Pascher, I.; Pearson, R. H.; Sundell, S. *Biochim. Biophys. Acta* **1981**, *650*, 21–51.

(16) Ghiggino, K. P.; Lee, A. G.; Meech, S. R.; O'Connor, D. V.; Phillips, D. *Biochemistry* **1981**, *20*, 5381–5389.

(17) (a) Fleming, P. J.; Koppel, D. E.; Lau, A. L. Y.; Strittmatter, P. *Biochemistry* **1979**, *18*, 5458–5464. (b) Ito, A. S.; de L. Castrucci, A. M.; Hruby, V. J.; Hadley, M. E.; Krajcarski, D. T.; Szabo, A. G. *Biochemistry* **1993**, *32*, 12264–12272. (c) Ladokhin, A. S.; Holloway, P. W. *Biophys. J.* **1995**, *69*, 506–517.

(18) (a) Schiffer, M.; Chang, C.-H.; Stevens, F. J. *Protein Eng.* **1992**, *5*, 213–214. (b) Kachel, K.; Ascuncion-Punzalan, E.; London, E. *Biochemistry* **1995**, *34*, 15475–15479.

(19) We have previously used a shorthand notation to designate complex crown ether structures. Using this system, 15-crown-5 is represented by (15) and 4,13-diaza-18-crown-6 is represented by H(N18N)H or simply (N18N). See: Hernandez, J. C.; Trafton, J. E.; Gokel, G. W. *Tetrahedron Lett.* **1991**, 6269–6272.

(9) (a) Tabushi, I.; Kuroda, Y.; Yokota, K. *Tetrahedron Lett.* **1982**, *23*, 4601–4604. (b) Menger, F. M.; Davis, D. S.; Persichetti, R. A.; Lee, J. J. *J. Am. Chem. Soc.* **1990**, *112*, 2451–2452. (c) Kobuke, Y.; Ueda, K.; Sokabe, M. *J. Am. Chem. Soc.* **1992**, *114*, 7618–7620. (d) Neevel, J. G.; Nolte, R. *Tetrahedron Lett.* **1984**, *25*(21), 2263–2266. (e) Nolte, R. J. M.; Beijnen, A. J. M.; Neevel, J. G.; Zwikker, J. W.; Verkley, A. J.; Drenth, W. *Israel J. Chem.* **1984**, *24*, 297–301. (f) Kragten, U. F.; Roks, M. F. M.; Nolte, R. J. M. *J. Chem. Soc., Chem. Commun.* **1985**, 1275–1276. (g) Jullien, L.; Lehn, J. *Tetrahedron Lett.* **1988**, *29*, 3803–3806. (h) Jullien, L.; Lehn, J. M. *J. Inclusion Phenom.* **1992**, *12*, 55–74. (i) Canceill, J.; Jullien, L.; Lacombe, L.; Lehn, J. M. *Helv. Chim. Acta* **1992**, *75*, 791–811. (j) Pregel, M.; Jullien, L.; Lehn, J. M. *Angew. Chem., Int. Ed. Engl.* **1992**, *31*, 1637–1639. (k) Pregel, M.; Jullien, L.; Canceill, J.; Lacombe, L.; Lehn, J. M. *J. Chem. Soc., Perkin Trans. 2* **1995**, 417–426. (l) Carmichael, V. E.; Dutton, P.; Fyles, T.; James, T.; Swan, J.; Zojaji, M. *J. Am. Chem. Soc.* **1989**, *111*, 767–769. (m) Fyles, T.; James, T.; Kaye, K. *Can. J. Chem.* **1990**, *68*, 976–978. (n) Fyles, T.; Kaye, K.; James, T.; Smiley, D. *Tetrahedron Lett.* **1990**, 1233. (o) Kaye, K.; Fyles, T. *J. Am. Chem. Soc.* **1993**, *115*, 12315–12321. (p) Fyles, T.; James, T.; Pryhicka, A.; Zojaji, M. *J. Org. Chem.* **1993**, *58*, 7456–7468. (q) Ghadiri, M. R.; Granja, J. R.; Buehler, L. K. *Nature* **1994**, *369*, 301–304. (r) Khazanovich, N.; Granja, J. R.; McRee, D. E.; Milligan, R. A.; Ghadiri, M. R. *J. Am. Chem. Soc.* **1994**, *116*, 6011–6012. (s) Stadler, E.; Dedek, P.; Yamashita, K.; Regen, S. *J. Am. Chem. Soc.* **1994**, *116*, 6677–6682. (t) Voyer, N.; Robitaille, M. *J. Am. Chem. Soc.* **1995**, *117*, 6599–6600. (u) Tanaka, Y.; Kobuke, Y.; Sokabe, M. *Angew. Chem., Int. Ed. Engl.* **1995**, *34*, 693–694. (v) Deng, G.; Merritt, M.; Yamashita, K.; Janout, V.; Sadownik, A.; Regen, S. L.; *J. Am. Chem. Soc.* **1996**, *118*, 3308. (w) Matsubara, A.; Asami, K.; Akagi, A.; Nishino, N. *Chem. Commun.* **1996**, 2069–2070. (x) Seebach, D.; Brunner, A.; Buerger, H. M.; Reusch, R. N.; Bramble, L. L. *Helv. Chim. Acta* **1996**, *79*, 507–517. (y) Wagner, H.; Harms, K.; Koert, U.; Meder, S.; Boheim, G. *Angew. Chem., Int. Ed. Engl.* **1996**, *35*, 2643–2646. (z) Matile, S. *J. Am. Chem. Soc.* **1997**, *119*, 8726–8727. (aa) Weiss, L. A.; Sakai, N.; Ghebremariam, B.; Ni, C.; Matile, S. *J. Am. Chem. Soc.* **1997**, *119*, 12142–12150. (bb) Meillon J.-C.; Voyer, N. *Angew. Chem., Int. Ed. Engl.* **1997**, *36*, 967. (cc) Pechulis, A. D.; Thompson, R. J.; Fojtik, J. P.; Schwartz, H. M.; Lisek, C. A.; Frye, L. B. *Biorg. Med. Chem.* **1997**, *5*, 1893–1901. (dd) Chen, L.; Sakai, N.; Moshiri, S. T.; Matile, S. *Tetrahedron Lett.* **1998**, *39*, 3627–3630. (ee) Clark, T. D.; Buehler, L. K.; Ghadiri, M. R. *J. Am. Chem. Soc.* **1998**, *120*, 651–656. (ff) Ni, C.; Matile, S. *Chem. Commun.* **1998**, 755–756. (gg) Reusch, R. N.; Sadoff, H. L. *Proc. Natl. Acad. Sci. U.S.A.* **1988**, *85*, 4176–4180.

(10) Nakano, A.; Xie, Q.; Mallen, J.; Echegoyen, L.; Gokel, G. W. *J. Am. Chem. Soc.* **1990**, *112*, 1287.

(11) Abel, E.; Fedders, M. F.; Gokel, G. W.; *J. Am. Chem. Soc.* **1995**, *117*, 1265–1270.

(12) (a) Hu, W.; Lee, K.-C.; Cross, T. A. *Biochemistry* **1993**, *32*, 7035. (b) Hu, W.; Cross, T. A. *Biochemistry* **1995**, *34*, 14147.

(13) (a) Gokel, G. W.; Dishong, D. M.; Diamond, C. J. *J. Chem. Soc., Chem. Commun.* **1980**, 1053. (b) Gokel, G. W. *Chem. Soc. Rev.* **1992**, *21*, 39–47.

(14) Roux, B.; MacKinnon, R. *Science* **1999**, *285*, 100–102.

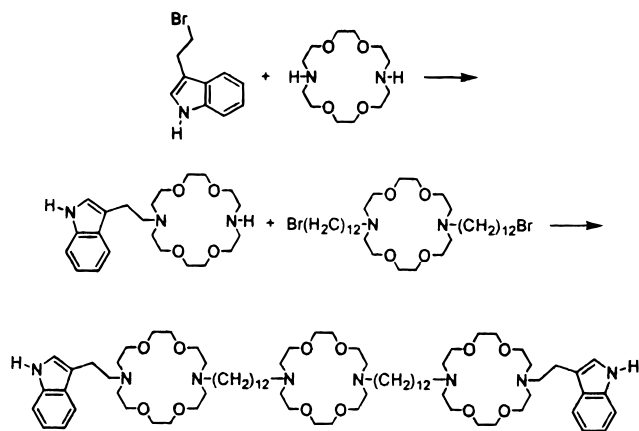


Figure 2. Synthetic scheme for the preparation of **1**.

18-crown-6 derivative terminated by dansyl residues, **6**, was prepared for use as a control compound.²⁰

Compound Syntheses. Of the eight structures studied, three were prepared particularly for this effort. They are $\text{InCH}_2\text{CH}_2\text{-(N18N)}\text{C}_{12}\text{(N18N)}\text{C}_{12}\text{(N18N)}\text{CH}_2\text{CH}_2\text{In}$, **1**, an analogue of **1** in which the indolyl nitrogen is methylated, **2**, and a dansyl-terminated derivative, $\text{Dn(N18N)}\text{C}_{12}\text{(N18N)}\text{C}_{12}\text{(N18N)}\text{Dn}$, **3**. The terminal substituents of indolyl derivatives **1** and **2** are attached via ethylene chains so the terminal nitrogen atoms in each case remain sp^3 hybridized. The dansyl group is attached to the terminal nitrogen atom by a sulfonamide residue. The terminal nitrogen in this case is nominally sp^2 hybridized. The sulfonated nitrogen atom is thus not expected to be protonated at physiological pH.

4-*N*-(2-(3-Indolyl)ethyl)-4,13-diaza-18-crown-6 was obtained in 38% yield by monoalkylation of diaza-18-crown-6 (Na_2CO_3 , KI, CH_3CN). The central fragment required for the coupling was also prepared from diaza-18-crown-6. The preparation of $\text{Br(CH}_2\text{)}_{12}\text{(N18N)(CH}_2\text{)}_{12}\text{Br}$, **A**, by treatment of H(N18N)H with $\text{Br(CH}_2\text{)}_{11}\text{COCl}$ to give $\text{Br(CH}_2\text{)}_{11}\text{CO(N18N)CO(CH}_2\text{)}_{11}\text{Br}$, followed by reduction ($\text{BH}_3\cdot\text{THF}$) has been previously reported.⁸ Alkylation of the monosubstituted crown by using **A** (Na_2CO_3 , KI, CH_3CN) afforded the hydrphile **1** (19%) as an oil that required repeated chromatography over silica to purify it (Figure 2).

The analogous tris(macrocycle) in which the indolyl nitrogen atom is methyl-substituted (**2**) was prepared by a similar sequence beginning with the *N*-methylated indole derivative. The sequence was otherwise similar, and the final alkylation to afford **2** was accomplished in 36% yield.

Likewise $\text{Dn(N18N)}\text{C}_{12}\text{(N18N)}\text{C}_{12}\text{(N18N)}\text{Dn}$, **3**, was prepared from $\text{H(N18N)}\text{C}_{12}\text{(N18N)}\text{C}_{12}\text{(N18N)}\text{H}$ and dansyl chloride to give **3** in 81% yield as a green oil.⁸ During the preparation of the monosubstituted crown, the disubstituted derivative $\text{Dn(N18N)}\text{Dn}$ (**4**) was isolated as a shiny, light green solid, mp 164–166 °C. A solid-state structure of **4** was obtained and has been reported separately.²⁰ Two additional, previously reported⁸ compounds are also discussed herein for comparative purposes. They are $\text{C}_{12}\text{(N18N)}\text{C}_{12}\text{(N18N)}\text{C}_{12}\text{(N18N)}\text{C}_{12}$, **5**, the “dodecyl channel”, and $\text{PhCH}_2\text{(N18N)}\text{C}_{12}\text{(N18N)}\text{C}_{12}\text{(N18N)}\text{CH}_2\text{Ph}$, **6**, the “benzyl channel”.

Membrane Structure. The synthetic channel was designed to function in a phospholipid bilayer. Typically, this involved insertion into vesicles made from a mixture of phosphatidylcholine (PC) and phosphatidylglycerol (PG) or from pure dioleoylphosphatidylcholine (DOPC). The former system was

Table 1. Assessment of Sodium Transport by Use of ^{23}Na NMR in a Phospholipid Bilayer

compd no.	compound structure	rel rate
	gramicidin	100
1	$\text{InCH}_2\text{CH}_2\text{(N18N)}\text{C}_{12}\text{(N18N)}\text{C}_{12}\text{(N18N)}\text{CH}_2\text{CH}_2\text{In}$	<2
2	$\text{Me-InCH}_2\text{CH}_2\text{(N18N)}\text{C}_{12}\text{(N18N)}\text{C}_{12}\text{(N18N)}\text{CH}_2\text{CH}_2\text{In-Me}$	23
3	$\text{Me}_2\text{NNpSO}_2\text{(N18N)}\text{C}_{12}\text{(N18N)}\text{C}_{12}\text{(N18N)}\text{SO}_2\text{NpNMe}_2$	24
4	$\text{Me}_2\text{NNpSO}_2\text{(N18N)}\text{SO}_2\text{NpNMe}_2$	<2
5	$\text{C}_{12}\text{(N18N)}\text{C}_{12}\text{(N18N)}\text{C}_{12}\text{(N18N)}\text{C}_{12}$	27
6	$\text{PhCH}_2\text{(N18N)}\text{C}_{12}\text{(N18N)}\text{C}_{12}\text{(N18N)}\text{CH}_2\text{Ph}$	39

used for most of the ^{23}Na NMR studies, but certain commercial samples of phospholipid monomers contained fluorescent impurities. In either case, the vesicles were prepared by the same method and laser light scattering found vesicles formed from either PC/PG or DOPC lipids to be about 2000 Å in diameter.

An important consideration for the present work is the overall thickness of the phospholipid bilayer and the width of the insulator regime or “hydrocarbon slab”. Work by Wiener and White²¹ on dioleoylphosphatidylcholine bilayers suggested that the insulator regime is ~34 Å. This agrees well with the solid-state data reported by Doyle and co-workers.⁴ The *n*-dodecyl chain, when fully extended, spans approximately 14 Å. The N–N distance known for 4,13-diaza-18-crown-6 derivatives is ~6 Å. This places the total $\text{C}_{12}\text{(N18N)}\text{C}_{12}$ distance at about 34 Å if the macrocycle is aligned with the lipid long axis. The molecular thickness of an alkyl chain is 5–7 Å and is therefore similar to the crown’s N–N span. The overall extension of this fragment would therefore be similar whether the central macrocoring is parallel or perpendicular to the bilayer surface.

Assessment of Sodium Transport by NMR. Two different methods were used to assess the efficacy of cation transport. One is the dynamic NMR method developed by Riddell and Hayer²² that is conducted in the phosphatidylcholine/phosphatidylglycerol vesicle system. Sodium cations trapped within the vesicles are distinguished from those in the bulk phase by use of a shift reagent (typically Dy^{3+}). A Na^+ cation transporter causes the line widths to alter. The variation can be quantitated, and a transport rate can be calculated. This methodology has been successfully applied to gramicidin.²³ In each of the NMR experiments reported here, the results are correlated to those obtained simultaneously for a standard compound (typically gramicidin) and normalized to a relative rate of 100.⁸ As conducted in our laboratory, the limit of detection in these experiments is approximately 2% of the transport rate of gramicidin. Previously reported⁸ exchange rate constants are dodecyl channel, **5**, 27 and benzyl channel, **6**, 39 relative to gramicidin (100).

The results of ^{23}Na NMR transport experiments are shown in Table 1. On the basis of the efficacy as ionophores of **5** and **6**, we fully expected indolylethyl derivative **1** to be active as well. We were, however, unable to detect any cation transport in the bilayer by the NMR method. In striking contrast, methylated derivative **2** transported Na^+ at a rate similar to that found previously for **5**. It was anticipated that dansyl crown **4** would be ineffective in the bilayer. Transport of cations by carriers is typically 3 orders of magnitude below that observed for channel-formers. The expectation that **4** would be a poor transporter under these conditions was intensified by the fact that the two nitrogen donor atoms are sp^2 hybridized, making

(21) Wiener, M. C.; White, S. H. *Biophys. J.* **1992**, *61*, 434–447.

(22) Riddell, F.; Hayer, M. *Biochim. Biophys. Acta* **1985**, *817*, 313–317.

(23) Buster, D.; Hinton, J.; Millett, F.; Shungu, D. *Biophys. J.* **1988**, *53*, 145–152.

(20) Meadows, E. S.; De Wall, S. L.; Salama, P. W.; Abel, E.; Gokel, G. W. *Supramol. Chem.* **1999**, *10*, 163–171.

them poor donors for cations. It was a question whether dansyl channel **3** would be a reasonable transporter since two of its six nitrogen atoms are likewise sp^2 hybridized. Its Na^+ ion transport rate was found to be similar to that of **2**, **3**, and **5** but lower than that of **6**. The complete absence of activity exhibited by **1** was surprising. An assessment of the reasons for the activity difference between **1** and **2** is presented below.

We have previously reported cation transport by these compounds as judged by the planar bilayer conductance (pbc) method.²⁴ Two problems attend the use of this technique from our perspective. First, neither the open–close frequency nor the measured conductance is readily convertible to a simple rate constant. Second, and more severe, while the pbc method is a subtle and sensitive technique, it is poorly reproducible, at least in our hands. The ²³Na NMR method provides an exchange rate constant that can be used to directly compare closely related compounds under essentially identical conditions.

Headgroup Positions for the Family of Tris(macrocycle) Channels. The best current evidence suggests the intravesicular conformation adopted by these compounds is as shown in Figure 1. The question we wished to address was whether we could obtain additional supporting evidence. We felt that an experimental assessment could be accomplished by using the fluorescence emission spectrum of dansyl channel **3**. The dansyl sidearms are shorter and more polar than those of dodecyl channel **5**. The sidearms are linked by a sulfonamide unit that is more rigid and less basic than a saturated amine. Notwithstanding these differences, the overall structure remains similar to those of **5** and **6**, and **3** is clearly functional as an ionophore (see Table 1).

The phospholipid bilayer can be thought of as having four polarity regimes. These are (1) the surface (water polarity), (2) the phosphoryl headgroup (high polarity), (3) the glyceryl esters (midpolar regime, medium polarity), and (4) the insulator regime (“hydrocarbon slab”). Measurement of CPK molecular models suggests that the $-(CH_2)_{12}(N18N)(CH_2)_{12}-$ fragment is approximately 40–42 Å long. If we use the hydrocarbon regime thickness value of 34 Å apparent in the recent MacKinnon structure,⁴ we anticipate that the dansyl residues will extend into the midpolar regime on each side of the bilayer. To our knowledge, no polarity value has been determined for this segment of the membrane. Even so, the polarity must be less than that on the water-contacting surface or in the headgroup region. Likewise, the insulator regime must exhibit a polarity essentially similar to that of a hydrocarbon. The dielectric constant (ϵ) for water is 81.5, and for hydrocarbons, ϵ is ~ 2 . In the present work, solvent polarity was expressed in terms of Reichardt’s (E_T) values,²⁵ which can be determined conveniently by experiment if required.

Fluorescence emission spectra were recorded for **3** in the specified solvents at $[3] = 1 \mu M$ using standard methods. The value of λ_{max} was then plotted (Figure 3) against the E_T polarity value (shown in parentheses): THF (37.4), CH_2Cl_2 (41.4), *n*-octanol (48.3), *n*-butanol (50.2), ethanol (51.9), and methanol (55.5).

The values observed for the fluorescence maxima were fitted by a linear function (slope = 1.08, $r^2 = 0.94$, six points). A similar correlation was observed when either Z or the dielectric constant (ϵ) was plotted on the abscissa. Dansyl channel **3** ($[3] = 1$ wt %) was then incorporated into phospholipid vesicles (see Experimental Section), and its fluorescence spectrum was

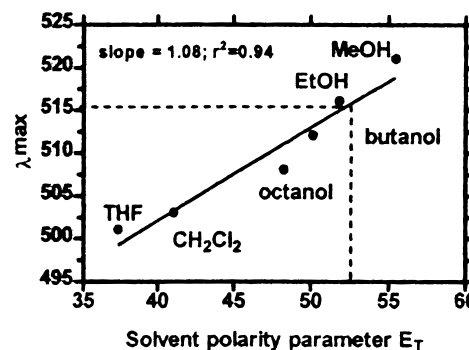


Figure 3. Plot of fluorescence emission maxima for **3** in solvents of differing polarity.

recorded. The maximum emission (λ_{max}) under these conditions was found to occur at 516 nm. Interpolation using the equation obtained from the graph allowed an E_T polarity value of 52.7 to be calculated. A separate plot of the four fluorescence maximum values obtained in alcohols (Figure 3) gave a steeper slope (1.8 vs 1.08) and a better fit ($r^2 = 0.98$ vs 0.94), but the overall line was used in the present calculation. Using the equation obtained graphically from all of the data, the parameter E_T at $\lambda = 516$ nm was calculated to be 53.3. The two values are thus within the range 53.0 ± 0.3 , an error range of less than 1%. This polarity value is intermediate between the E_T parameters for CH_3OH (55.5) and CH_3CH_2OH (51.9).

The fluorescence behavior of *N,N'*-didansyl-4,13-diaza-18-crown-6 (Dn(N18N)Dn, **4**) was similarly assessed in a variety of solvents.²⁰ The crown is expected to serve as a carrier rather than as a channel. Thus, on average, it is expected to spend more time in the nonpolar regime than proximate to the headgroups. The emission maximum for **4** in phospholipid bilayer vesicles was found to be 510.8 ± 0.7 nm. This is intermediate in polarity between butanol and propanol rather than between methanol and ethanol and corresponds well to the polarity data reported by Zacharlasse *et al.*²⁶

The E_T polarity value of 53 for **3** seems reasonable because the spectroscopic studies have shown that the Stern layer of a micelle has an environment similar to that of methanol or ethanol.²⁷ Studies conducted by others using vesicular membranes in which dansyl-substituted lipid monomers were incorporated showed a fluorescence shift similar to the one we observed.²⁸ These data not only seem reasonable for the midpolar regime but they also clearly show that the headgroups are not embedded in the far less polar lipid environment. The results presented here are strongly suggestive, but we recognize that there is an assumption in correlating the fluorescence shift with solvent polarity. It is that the solvent molecules relax faster than the lifetime of the excited state of the fluorophore. It is difficult to determine whether relaxation inside a phospholipid bilayer occurs on this time scale. In addition, the carbon chains of bilayer lipids are least ordered near the midplane.²⁹ The fluorophore in a bilayer thus encounters gradients in rigidity as well as polarity.

Fluorescence Depth Quenching. The sensitivity of dansyl fluorescence to the polarity of its environment is an excellent

(26) Zacharlasse, K. A.; Phuc, N. V.; Kozankiewicz, B. *J. Chem. Phys.* **1981**, *85*, 2676–2683

(27) Fendler, J. H. *Membrane Mimetic Chemistry*; John Wiley & Sons: New York, 1982; p 19.

(28) (a) Stubbs, C. D.; Meech, S. R.; Lee, A. G.; Phillips, D. *Biochim. Biophys. Acta* **1985**, *815*, 351. (b) Chen, R. F. *Arch. Biochem. Biophys.* **1967**, *120*, 609.

(29) *Biological Membranes: A Molecular Perspective from Computation to Experiment*; Merz, K. M. Jr., Roux, B., Eds.; Birkhäuser: Boston, 1996; p 593.

(24) Murillo, O.; Abel, E.; Maguire, G. E. M.; Gokel, G. W. *J. Chem. Soc., Chem. Commun.* **1996**, 2147–2148.

(25) Reichardt, C. *Solvents and Solvent Effects in Organic Chemistry*, 2nd ed.; Verlag Chemie, Weinheim, 1988; p 366.

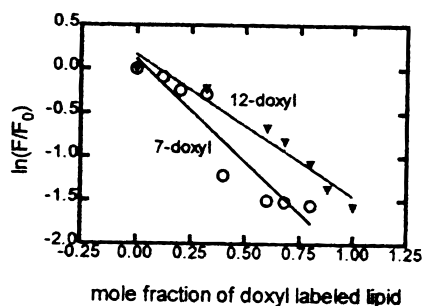
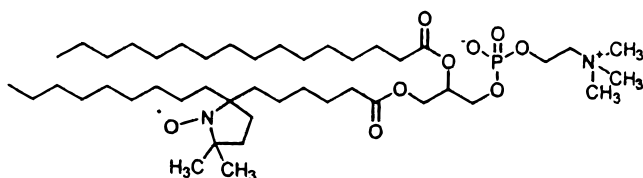


Figure 4. Fluorescence depth quenching for **3** with 7- and 12-doxyl lipids.

means for assessing the position of the headgroup. A drawback is the lack of precision in assigning polarity values to the bilayer's various regimes. A complementary approach for assessing structural relationships is to use doxyl-substituted phospholipids as intramembrane fluorescence quenchers.³⁰

Two commercially available compounds³¹ were chosen for the present studies. Both were phosphatidylcholine derivatives having palmitoyl tails. In each case a 2,2-dimethylpyrrolidine *N*-oxide was spiro-fused in its four position to either the 7- or 12-position of the palmitoyl chain. The 7-doxyl lipid is illustrated.



Mixtures of distearoyl phosphatidylcholine and one of the spin-labeled lipids were prepared at mole fractions ranging from 0 to 1. Vesicles were prepared by sonication in the usual fashion (see Experimental Section). Dansyl channel **3** was added to the vesicle suspension to a final concentration of 1×10^{-6} M. The fluorescence spectrum of **3** was then determined in each lipid mixture. Figure 4 shows plots of $\ln(F/F_0)$ as a function of mole fraction for each of the lipid mixtures. The straight-line relationship for the 12-doxyl system is excellent, having $r^2 = 0.95$ (7 points). The quality of the data for the 7-doxyl system is poorer but still acceptable ($r^2 = 0.89$, 7 points).

The Perrin equation (shown) was used to determine the distance of the fluorescent probe from the center of the bilayer. The assumption is that the fluorophore and the quencher are located in parallel planes separated by a vertical distance (Z)

$$\ln \frac{F}{F_0} = \frac{-\pi C}{70} (R_0^2 - X^2 - Z^2)$$

in which F and F_0 are the quenched fluorescence and the fluorescence at zero quencher concentration, C is the molar ratio of spin-labeled lipid, R_0 is the critical quenching radius, X is the closest allowed lateral approach, and Z is the vertical distance between the fluorophore and the quencher. The plot of $\ln(F/F_0)$ vs C (Figure 4) gave a straight line with a slope equal to $(\pi/70)m$, where $m = (R_0^2 - X^2 - Z^2)$. The coefficients were determined by linear regression analysis.³² Assuming that R_0 and X are constant for a given quencher-fluorophore pair, subtraction of the value $(R_0^2 - X^2 - Z^2)$ obtained for a quencher

(a) from the $(R_0^2 - X^2 - Z^2)$ value obtained for a second quencher (b) will give the difference $(Z_a^2 - Z_b^2)$. Once this difference is known, the distance from the center of the bilayer (P) can be calculated as

$$P = \left(\frac{Z_b^2 - Z_a^2 + Q_a^2 - Q_b^2}{2(Q_a - Q_b)} \right)$$

where Q_a and Q_b are the distance from the center of the bilayer of quencher a and quencher b. The distances specified in the literature³³ from the center of the bilayer for the 7-doxyl and 12-doxyl lipids are 10 and 5.9 Å, respectively. The values of m obtained when the 7-doxyl and the 12-doxyl lipids were used were 31.35 ± 1.86 and 47.78 ± 4.12 , respectively. Using the Q_a and Q_b values for the 7-doxyl and 12-doxyl lipid pair, we determined that our dansyl-labeled headgroup lies at approximately 14 Å from the center of the bilayer. This value means that the two dansyl headgroups are separated by 28 Å, approximately the thickness of the hydrocarbon slab. The value is consistent with the headgroup being at or near the midpolar regime of the membrane. There is some ambiguity in this distance value because the dansyl group's naphthalene is approximately 5 Å wide and the distance from the sulfonyl S to the dimethylamino N is ~6 Å. Addition of 5–6 Å places the headgroups at a separation of 38–40 Å or exactly the span suggested by CPK models for the extended conformation.

Indolyl-Terminated Tris(macrocycle) Channels. The indolyl residue is the aromatic component of tryptophan's side chain. The rarest of the common amino acids,³⁴ tryptophan often occurs in proteins³⁵ and peptides¹² at or near the membrane's aqueous margin. Indeed, alkyl-substituted indoles form stable vesicles if the alkyl group is long enough and suitably placed on the indole nucleus.¹¹ Moreover, the fluorescence behavior of indole in tryptophan has been used extensively in biology, for example as a probe to assess the position of this residue in proteins embedded in a bilayer membrane.³⁶ We thus incorporated the indolethyl side chain at each terminus of the tris-(macrocycle) system. A potential drawback was apparent from an examination of CPK molecular models: it appeared that a hydrogen bond could readily form between the indolyl N-H and one of several macrocyclic oxygen atoms. The existence of such a hydrogen bond would position indole directly over the channel's putative entry orifice and thus block it. Whether or not the formation of such a hydrogen bond(s) was sufficient to block the pore was unknown, but the possibility was clearly a concern.

Hydrogen bond formation appeared from CPK models to hold the indole in a relationship approximately perpendicular to the plane of the macrocyclic. This structural possibility was further explored by computational modeling. We chose to model only the headgroup fragment of indolyl channel **1**, namely InCH_2 -

(33) (a) Oldfield, E.; Meadows, M.; Rice, D.; Jacobs, R. *Biochemistry* **1978**, *17*, 2727. (b) Zaccari, G.; Buldt, G.; Seelig, J.; Seelig, A. *J. Mol. Biol.* **1979**, *134*, 693. (c) Caffrey, M.; Feigenson, G. W. *Biochemistry* **1981**, *20*, 1949. (d) Lewis, B. A.; Engelman, D. *J. Mol. Biol.* **1983**, *166*, 211.

(34) Creighton, T. E. *Proteins: Structures and Molecular Properties*, 2nd ed.; W. H. Freeman and Co.: New York, 1993; p 4.

(35) Hu, W.; Lee, K.-C.; Cross, T. A. *Biochemistry* **1993**, *32*, 7035–7047.

(36) (a) Cowgill, R. W. *Biochim. Biophys. Acta* **1967**, *133*, 6. (b) Surewicz, W. K.; Epand, R. M. *Biochemistry* **1984**, *23*, 6072. (c) McKnight, C. J.; Rafalski, M.; Gierasch, L. *Biochemistry* **1991**, *30*, 6241. (d) Chung, L. A.; Lear, J. D.; DeGrado, W. F. *Biochemistry* **1992**, *31*, 6608. (e) Ito, A. S.; Castrucci, A. M. de L.; Hruby, V. J.; Hadley, M. E.; Krajcarski, D. T.; Szabo, A. G. *Biochemistry* **1993**, *32*, 12264. (f) Ladokin, A. S.; Holloway, P. A.; *Biophys. J.* **1995**, *69*, 506. (g) Kachel, Kelli; Asuncion-Punzalan, E.; London, E. *Biochemistry* **1995**, *34*, 15475.

(30) Chattopadhyay, A.; London, E. *Biochemistry* **1987**, *26*, 39.

(31) Avanti Polar Lipids, Alabaster, AL.

(32) Chung, L. A.; Lear, J. D.; DeGrado, W. F. *Biochemistry* **1992**, *31*, 6608.

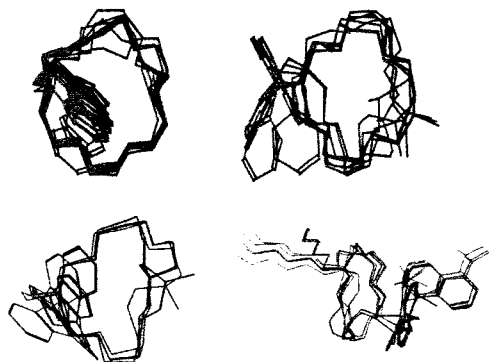


Figure 5. Monte Carlo simulations for the sidearm-crown-*n*-hexyl fragments of (a) **1**, (b) **8**, (c) **2**, and (d) **3**.

$\text{CH}_2(\text{N18N})(\text{CH}_2)_5\text{CH}_3$. This structure was subjected to the Monte Carlo search routine of MacroModel (CHCl₃ solvation model).³⁷ Calculations were also undertaken for the corresponding headgroup fragment $\text{PhCH}_2(\text{N18N})(\text{CH}_2)_5\text{CH}_3$ of the functional benzyl analogue **6**, $\text{PhCH}_2(\text{N18N})\text{C}_{12}(\text{N18N})\text{C}_{12}(\text{N18N})\text{CH}_2\text{Ph}$. The Monte Carlo conformational search calculations were performed over 10^6 cycles in each case and ultimately afforded numerous low energy structures. The 10 lowest energy structures (superimposed, all within 1 kcal of the global minimum) for fragments of **1** and **6** are overlaid in panels a and b of Figure 5. Similar calculations using a water solvation model gave essentially the same results. All of the calculated low energy conformers of **1** were transannularly H-bonded, as anticipated from the CPK models. In practice, this is expected to occlude the molecular orifice. In contrast, the *N*-benzyl group of the **6** fragment is turned away from the opening in all of the lowest energy conformers.

The H-bonding potential of **1** may be eliminated by methylating the indolyl nitrogen atom (**2**). Monte Carlo simulations for the headgroup fragment of *N*-methylindole channel **2** (Figure 5, panel c) are similar to those of **6** and suggest blockade of the channel's entrance. Simulations conducted for the corresponding fragment of dansyl channel **3** indicated that the structure is, like the benzyl fragment, relatively flexible. In all of the lowest energy structures, the dansyl group was located on one face of the macrocyclic ring and the alkyl chain was on the other face. This is reminiscent of the recently reported solid-state structure for the bis(dansyl) crown **4**.²⁰

Experimental confirmation of H-bond formation was obtained by examining the infrared spectrum of **2** in CCl₄ at concentrations ranging from 10 to 100 μM . The only vibration apparent in the 3000–2000 cm^{-1} range was a sharp doublet observed at 2927 ± 1 and 2855 ± 1 cm^{-1} that was not altered either in position or shape by a 100-fold concentration change. In contrast, the infrared spectrum of 3-(2-*N,N*-dimethylamino)-indole exhibits a single, broad band ranging from 3000 to 2850 cm^{-1} .³⁸

It should also be noted that the line-angle representations mask the ~ 3.4 Å thickness of the aromatic residue. The linear N–N distance in diaza-18-crown-6 is approximately 5.5 Å.³⁹ Thus, the potential for blocking the crown's orifice is significant.

(37) MacroModel v. 5.0, Department of Chemistry, Columbia University, New York, 10027. All carbon–carbon bonds of the *N*-hexyl group were constrained to the anti conformation.

(38) Pouchert, C. J. *The Aldrich Library of Infrared Spectra*, 2nd ed.; Aldrich Chemical Co.: Milwaukee, WI, 1975; p 1083E.

(39) (a) Medina, J. C.; Goodnow, T. T.; Bott, S.; Atwood, J. L.; Kaifer, A. E.; Gokel, G. W. *J. Chem. Soc., Chem. Commun.* **1991**, 290–292. (b) Medina, J. C.; Goodnow, T. T.; Rojas, M. T.; Atwood, J. L.; Lynn, B. C.; Kaifer, A. E.; Gokel, G. W. *J. Am. Chem. Soc.* **1992**, *114*, 10583–10595.

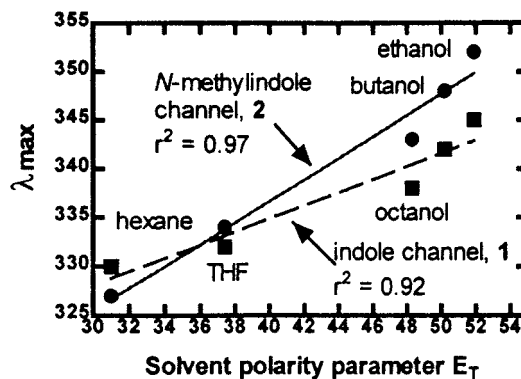


Figure 6. Plot of fluorescence emission maxima for **1** and **2** in solvents of differing polarity.

The Na⁺ transport data shown in Table 1 demonstrate that **1** is completely ineffective as a channel model. In contrast, the methylindolyl channel (**2**) and the dodecyl-sidearmed analogue (**5**) function about equally well. The failure of **1** to conduct cations was disappointing but important. Blockage of a pore by the formation of a hydrogen bond suggests considerable order of the headgroup structure. Moreover, compounds **1** and **2** are nearly identical in every respect. Their respective molecular weights are 1378 and 1406, a difference of less than 2%. Despite the near identity in size, shape, polarity, and molecular weight, **2** effectively transports Na⁺ in a phospholipid bilayer while **1** is inactive.

Fluorescence Behavior of the Indolyl Channels. The fluorescence emission spectrum of inactive **1** was determined in various solvents and in the phospholipid bilayer of stable vesicles. The fluorescence maximum for **1** ranged from 330 nm in hexane to 345 nm in anhydrous ethanol solution. A plot of the solvent dependence of the emission maximum for **1** vs E_T ²⁵ ($r^2 = 0.92$) is shown in Figure 6. The fluorescence maximum observed for **1** in phospholipid vesicles was 334 nm. This corresponds to an average polarity (E_T) experienced by the indole groups of 38.7, which is less than that for *n*-octanol and near that of THF. The headgroups experience a nonpolar environment rather than one similar to that of ethanol as observed for dansyl channel **3**. This suggests that the “channel” is not in a fully extended conformation but in what might be called a “globular” arrangement. This would be expected if the macrocycle headgroup is blocked by H-bonding and its ability to interact with water is impeded. It would then be ineffective either as a headgroup or as an entry portal, and the extended conformation would likely collapse to a globular arrangement. We attribute the lack of ionophoretic activity to the combination of H-bond blockade of the putative pore and the resulting “globular” conformation in which the tris(macrocycle) does not span the bilayer.

A similar study was undertaken with *N*-methylindolyl channel **2**. The data fit (Figure 6) was better ($r^2 = 0.97$) than that for the indolyl channel, and the sensitivity of the fluorescence maximum to polarity was greater (range: 327–352 nm). In a phospholipid bilayer, $\lambda_{\text{max}} = 343$ nm, identical to the fluorescence maximum observed in butanol. Using the coefficients obtained from the graph, the polarity parameter (E_T) was calculated to be 45.8, which places the polarity experienced by the headgroups of **2** slightly lower than that for butanol but far above those of **1**.

Fluorescence Energy Transfer Experiments. An interesting and important question concerning the tris(macrocycle) channel design is whether these compounds act within the bilayer as monomers to transport cations. It is possible that the tris-

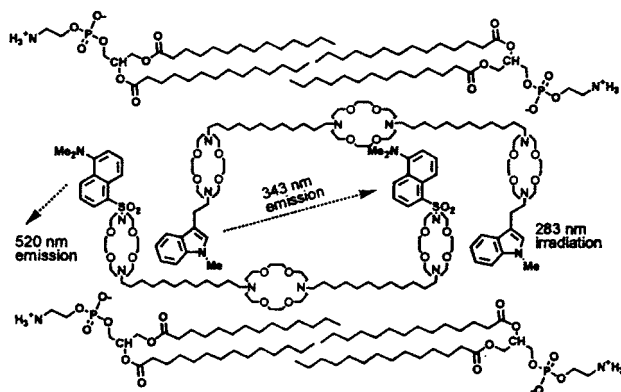


Figure 7. Schematic of the fluorescence energy transfer experiment involving compounds **2** and **3** in the phospholipid bilayer.

(macrocyclic) channels function by forming an aggregate as some channel-forming peptides and proteins are thought to do. Such association might correspond, for example, to the barrel-stave model that has been proposed for alamethicin.^{17a} The availability of compounds **2** and **3** afforded an opportunity to experimentally assess the aggregation state.

Two types of aggregates can be envisioned—homooligomers and heterooligomers. In the former case, these would comprise 2_n and 3_n but not $(2_x \cdot 3_y)$. We envision these as cylindrical aggregates that form pores. While we see no a priori reason to imagine that homooligomers would be more or less favored than heterooligomers, we cannot strictly rule out either possibility. We have, however, attempted to assess the overall aggregation situation using methods that have previously been applied to natural systems. Indeed, energy transfer between dansyl and indolyl has been assessed in bilayers when these two residues were at opposite ends of amide-containing hydrocarbon spacers.⁴⁰ In the present case, energy transfer is anticipated between dansyl and *N*-methylindolyl. It is reported that *N*-methylindole is less prone to self-quench than is the corresponding *N*-H compound.⁴¹

The fluorescence maximum observed for *N*-methylindolyl derivative **2** was 343 nm. This is essentially the wavelength at which dansyl channel **3** absorbs light. Thus, the wavelengths are appropriate for energy transfer to occur between **2** (absorption 283 nm, fluorescence 343 nm) and **3** (absorption 340 nm) (Figure 7). Energy transfer (from **2** to **3**) could be detected as emission at 520 nm. If the channel compounds aggregate in the lipid bilayer, the resulting proximity of the aromatic moieties should cause an increase in the fluorescence intensity of dansyl channel **3** when the *N*-methylindole channel **2** is irradiated. At the same time, the fluorescence of *N*-methylindole would be quenched.

Our strategy was to study a phospholipid liposome system containing a mixture of **2** and **3**. In all cases, $[2] + [3] = (1 \times 10^{-5} \text{ M})$ and the mole fraction varied from $0 \rightarrow 1$ for **2** while the mole fraction of **3** varied from $1 \rightarrow 0$ ($30 \mu\text{L}$ total aliquots of a 1 mM stock solution of each, ultimately diluted to 3 mL: 30:0, 25:5, 20:10, 15:15, 10:20, 5:25, and 0:30). Thus, the molar ratio of indole to dansyl channel was varied from 1, 0.83, 0.66, 0.5, 0.33, 0.16 to zero, while the total concentration of channel remained constant. Three sets of fluorescence measurements were performed. First, each sample was irradiated at 283 nm. In each sample containing **2**, a typical emission profile was observed with $\lambda_{\text{max}} = 340 \text{ nm}$. Second, each sample was

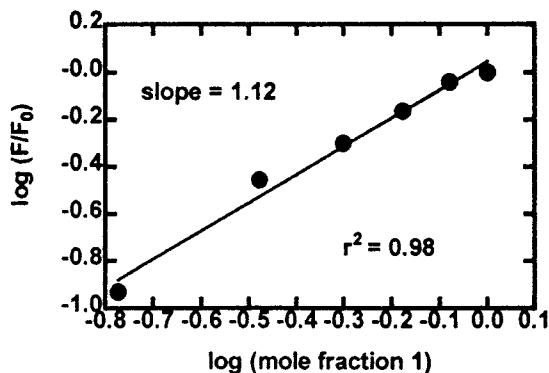


Figure 8. Plot of $\log F/F_0$ vs $\log(\text{mole fraction of } 3)$.

irradiated at 340 nm. Samples containing dansyl channel **3** fluoresced at $\lambda_{\text{max}} = 520 \text{ nm}$. Third, all samples were irradiated at 283 nm and their fluorescence emission spectra were recorded between 460 and 560 nm. In the latter experiments, a weak fluorescent band was observed that corresponded to dansyl channel (**3**) emission when the system was irradiated at the absorption maximum of *N*-methylindole channel (**2**, 283 nm). This band was not due to energy transfer; rather, it was attributed to the dansyl groups' ability to absorb some radiation at this wavelength. A sample containing only the dansyl channel ($[3] = 1 \times 10^{-6} \text{ M}$) in phospholipid vesicles and irradiated at 283 nm showed the same weak fluorescent band. In all cases involving phospholipid vesicles (even in the absence of **2** or **3**), a sharp diffraction peak was observed at $\lambda_{\text{max}} = 565 \text{ nm}$.

The key finding of these studies is that over the concentration range studied, the fluorescence behavior of either **2** or **3** appears to be independent. Neither self-quenching nor fluorescence energy transfer is observed for these compounds. The plot of $\log F/F_0$ vs \log mole fraction for *N*-methylindole channel **2** is shown in Figure 8. Assuming that energy transfer could occur if the monomers were proximate and assuming that energy transfer is efficient, the slope of the line will be related to the aggregation state of the monomers.⁴² The inference we draw from the spectral evidence and the graphical relationship shown is that there is no evidence for aggregation.

Conclusions

Three novel tris(macrocylic) channels have been prepared that have fluorescent residues at their distal termini. The solvent dependence of the fluorescence maximum was used to determine that the dansyl and methylindolyl headgroups of channels **2** and **3** experienced a methanol–ethanol-like polarity in the phospholipid bilayer. This suggested that the channel headgroups were positioned near the bilayer's midpolar regime. Indolyl-terminated channel **1** was shown to be intramolecularly H-bonded and not to exhibit ionophoretic activity. The lack of activity observed for **1** appears to be due an H-bond blockade of the crown, which reduces the latter's polarity and leads to a globular, non-channel-like conformation. Fluorescence depth quenching showed that the dansyl groups of **3** were 14 \AA from the midplane of the bilayer or 28 \AA apart. This is in accord with an extended conformation and residence of these groups in the midpolar regime. Fluorescence energy transfer between **2** and **3** suggested that each of these channels was monomeric in the bilayer. These fluorescence studies all comport with the channel structure illustrated schematically in Figure 1.

(40) Gryczynski, I.; Wicz, W.; Johnson, M. L.; Cheung, H. C.; Wang, C.-K.; Lakowicz, J. R. *Biophys. J.* **1988**, *54*, 577–586.

(41) Horrocks, D. L. *J. Chem. Phys.* **1969**, *50*, 4151–4156.

(42) (a) London, E.; Khorana, G. *J. Biol. Chem.* **1982**, *257*, 7003. (b) Veatch, W. R.; Stryer, L. *J. Mol. Biol.* **1977**, *113*, 89. (c) Vanderkooi, J. M.; Ierokomas, K., Jr.; Ikegami, A. *Biochemistry* **1977**, *16*, 1263.

Experimental Section

^1H NMR spectra were recorded at either 300 or 500 MHz in CDCl_3 unless otherwise specified. Chemical shifts are given in ppm (δ) downfield from internal TMS. NMR data are recorded as follows: chemical shift, peak multiplicity (b = broad; s = singlet; d = doublet; t = triplet; m = multiplet, bs = broad singlet, etc.), integration, and assignment. Infrared spectra were recorded on a Fourier transform infrared spectrophotometer (in KBr unless otherwise noted) and were calibrated against the 1601 cm^{-1} band of polystyrene. Fluorescence intensities were measured on a Hitachi 650-10M fluorescence spectrometer (excitation 450 nm, emission 510 nm) and were obtained using 2.5 mm slits on both the excitation and emission sides. The pH of the buffer solutions was adjusted and monitored by means of a HORIBA M-8 pH Meter. Melting points were determined on a Thomas-Hoover apparatus in open capillaries and are uncorrected. Thin layer chromatographic (TLC) analyses were performed on aluminum oxide 60 F-254 neutral (type E, 0.2 mm thickness), Merck. Preparative chromatography columns were packed with alumina [neutral, Brockman 1, standard grade (150 mesh, Aldrich)], Sephadex LH-20, or silica gel (Merck, 230–400 mesh, 60C).

All reactions were conducted under dry N_2 unless otherwise noted. All reagents were the best grade commercially available and were distilled, recrystallized, or used without further purification, as appropriate. Molecular distillation temperatures refer to the oven temperature of a Kugelrohr apparatus. Combustion analyses were performed by Atlantic Microlab, Inc., Atlanta, GA, and are reported as percents.

Measurement of Cation Transport Rates by ^{23}Na NMR. (a) Vesicle Preparation. Phosphatidylcholine (chloroform–methanol solution), phosphatidylglycerol (CHCl_3 –MeOH solution), Na_2HPO_4 , NaH_2PO_4 , KH_2PO_4 , NaCl (molecular grade reagents), gramicidin D (85% gramicidin A, 15% gramicidin B and C), and sodium tripolyphosphate (90–95%) were purchased from Sigma, St. Louis, MO, and used without further purification. Diethyl ether (anhydrous, Mallinckrodt) was distilled over Na^0 /benzophenone prior to use. Distilled, deionized water was used to prepare the buffer solution. 2,2,2-Trifluoroethanol (TFE), NMR grade, $\text{DyCl}_3 \cdot 6\text{H}_2\text{O}$ (99.99%), D_2O , KCl (ACS grade), and CHCl_3 (HPLC grade) were purchased from Aldrich and used without further purification. The sonication was done using either a Branson model 1200 or Branson 12 water bath. The mean diameters of the vesicles were determined by using a Coulter N4SD submicron particle analyzer.

To prepare the vesicles, the procedure described by Papahadjopoulos⁴³ was followed with certain modifications. The concentration of Na^+ in the phosphate-buffered saline solution (1:10 dilution) was increased by addition of NaCl until $[\text{Na}^+]_{\text{total}} = 100\text{ mM}$. Phosphatidylglycerol (PtdGro) and phosphatidylcholine (PtdCho) solutions were allowed to reach room temperature before utilization. A solution of phosphatidylglycerol (1.30 mL) and phosphatidylcholine (0.52 mL) was diluted in a volumetric flask to 25.00 mL with CHCl_3 . This solution was poured into a 250 mL round-bottomed flask, and the solvent was evaporated in vacuo. The system was maintained under vacuum ($<0.02\text{ mmHg}$) overnight, and then it was purged with nitrogen. The film of lipids was dissolved in 25.0 mL of ether, and 10.00 mL of a buffered saline solution (1:10 dilution) was added.

The resulting two-phase suspension was sonicated at 2–5 °C in a water bath sonicator for 40 min. All of the organic phase was removed by rotary evaporation as described in the sequence following. The rotary evaporator was gradually evacuated by reducing the pressure sequentially as follows: $\sim 500\text{ mm}$ for 10 min (no heating), $\sim 200\text{ mm}$ (10 min, no heat), then warm in a 40 °C water bath (~ 30 – 60 s), then remove water bath, and evacuate (high vacuum, $\sim 5\text{ min}$, solution becomes translucent). The resulting vesicle solution was either filtered through a polycarbonate membrane (Poretics, 0.4 micron) or centrifuged for 15 min. Vesicle size was determined by laser light scattering. The sample was diluted in the cuvette to a concentration appropriate for the instrument using 1:10 buffer (see below). This preparation produces vesicles with an average diameter of 175–200 nm ($\sim 2000\text{ \AA}$).

Integration of the ^{23}Na signals inside and outside the vesicle showed $\sim 3\%$ aqueous volume entrapment.

(b) Buffer Composition. The composition of the buffered saline solution employed to prepare the 1:10 buffered saline solution was as follows: NaCl (13.804 mmol, 0.80064 g), KCl (0.26 mmol, 0.01936 g), Na_2HPO_4 (0.64 mmol, 0.09088 g), and KH_2PO_4 (0.1399 mmol, 0.01904 g) were diluted to 100 mL with H_2O at pH 7.3 (25 °C). A 10.0 mL aliquot of the stock solution was taken, and NaCl was added (8.5 mmol, 0.4979 g). The solution was diluted to 100 mL with distilled water. The total Na^+ concentration in the final buffer solution was 100 mM.

(c) Insertion of Ionophores. Ionophores were inserted into the membranes either during vesicle formation or after vesicle preparation had been completed. When the vesicles were prepared as described above, a $\text{CF}_3\text{CH}_2\text{OH}$ solution of the ionophore (~ 0.5 – 1 mM) was added in an amount appropriate to afford the required 5–40 μM concentration. A mixture of the vesicle and $\text{CF}_3\text{CH}_2\text{OH}$ solution in an Eppendorf vial was warmed at 60 °C (water bath) for 1 h. This solution was then transferred to an NMR tube for study. Preparation of samples directly in 5 mm NMR tubes was normally successful but vortexing the Eppendorf vials generally produced more homogeneous samples.

Alternately, the vesicle preparation described above could be conducted in the presence of the $\text{CF}_3\text{CH}_2\text{OH}$ solution of ionophore. In this way, different concentrations of ionophore could be incorporated directly during vesicle formation. Thus, prior to formation of the vesicles, an amount of ionophore suitable to give the desired final concentration (in $\text{CF}_3\text{CH}_2\text{OH}$) was added to the vesicle preparation solution. Vesicles were prepared in the normal way, and ionophore concentrations were calculated on the basis of the assumption that no material was lost during vesicle preparation. Vesicles containing **7** were prepared by both methods and data obtained were within experimental error.

(d) Shift Reagent. The shift reagent was prepared by mixing an aliquot of 2.00 mL of a tripolyphosphate solution (0.200 M) and 1.00 mL of a Dy^{3+} solution (0.100 M). No correction for reagent purity was made in the case of the tripolyphosphate.

(e) NMR Measurements. ^{23}Na NMR spectra were obtained on an NMR spectrometer operating either at 132.2 or 79.4 MHz (equivalent to 500 or 300 MHz for ^1H). Chemical shifts were measured as differences between the frequency values for Na^+ inside and outside of the vesicle. Upfield shifts were defined as negative. Samples for NMR measurements were prepared in Eppendorf vials (1.7 mL) and then transferred to 5 mm NMR sample tubes. After the incubation period (see above), the samples were cooled to room temperature and then diluted with 0.100 mL of D_2O and 0.100 mL of shift reagent solution (D_2O lock). The solution was then allowed to equilibrate for at least 1 h before data acquisition. Typically, 240 FID transients were accumulated per data set at a probe temperature of 25 °C.

(f) Rate Constants. Once the potential ionophore was incorporated into the vesicles, any line-broadening of the ^{23}Na signal was determined. In the slow exchange region, the rate constant, $k = 1/\tau$, is directly proportional to the observed line broadening, $= \pi(\Delta\nu - \Delta\nu_0)$. The rate constant is determined from the slope of a plot of $1/\tau$ vs ionophore concentration.

***N,N'*-Bis[12-[*N'*-(2-(3-indolyl)ethyl)diaza-18-crown-6]dodecyl]-diaza-18-crown-6, $\text{InCH}_2\text{CH}_2(\text{N18N})\text{C}_{12}(\text{N18N})\text{C}_{12}(\text{N18N})\text{CH}_2\text{CH}_2\text{In}$, **1**. (a) $\text{In}(\text{CH}_2)_2(\text{N18N})\text{H}$.** A solution of diaza-18-crown-6 (3.15 g, 12.0 mmol), 3-(2-bromoethyl)indole (2.29 g, 10.2 mmol), Na_2CO_3 (25.44 g, 240 mmol), and KI (0.25 g, 1.5 mmol) in MeCN (120 mL) under N_2 was heated to reflux for 78 h. The mixture was cooled, filtered, and concentrated. The resulting oil was washed with H_2O ($3 \times 50\text{ mL}$), extracted with CH_2Cl_2 (100 mL), dried (MgSO_4), and filtered, and the crude product was purified by column chromatography (alumina, 1–30% *n*-PrOH/ CH_2Cl_2). The fractions containing the desired product were rechromatographed (silica gel, 10% $\text{Et}_3\text{N}:\text{Me}_2\text{CO}$) to give $\text{In}(\text{CH}_2)_2(\text{N18N})\text{H}$ (1.575 g, 38%) as a dark brown oil: ^1H NMR 1.2 (d, *n*-PrOH contaminant), 2.85 (m, 10 H, $\text{NCH}_2\text{CH}_2\text{In}$, $\text{NCH}_2\text{CH}_2\text{O}$), 3.6 (m, 18 H, $\text{NCH}_2\text{CH}_2\text{O}$, $\text{NCH}_2\text{CH}_2\text{Ind}$), 4.0 (m, *n*-PrOH), 7.06 (m, 3 H, aromatic), 7.32 (d, $J = 4.8$, aromatic), and 7.55 (d, $J = 4.8$, aromatic); mass spectrum (ESI) $[\text{M} + \text{H}]^+ = 407.5$. The sample was used directly in the next step.

(43) Szoka, F.; Papahadjopoulos, D. *Proc. Natl. Acad. Sci. U.S.A.* **1978**, *75*, 4194–4198.

(b) **InCH₂CH₂(N18N)C₁₂(N18N)C₁₂(N18N)CH₂CH₂In.** A solution of InCH₂CH₂(N18N)H (1.575 g, 3.88 mmol), Br(CH₂)₁₂(N18N)(CH₂)₁₂-Br (1.469 g, 1.94 mmol), Na₂CO₃ (4.11 g, 38.8 mmol), and KI (0.047 g, 0.28 mmol) in MeCN (40 mL), under N₂, was heated at reflux for 24 h. The reaction mixture was cooled (rt), filtered, and concentrated in vacuo. The resulting residue was washed with water (3 × 40 mL), extracted with CH₂Cl₂ (100 mL), dried (MgSO₄), filtered, and concentrated, and the crude product was purified by column chromatography [silica gel; Me₂CO, 1% Et₃N:Me₂CO (v/v)]. The major fraction (*R_f* = 41/64) was rechromatographed [alumina, grade II; 5% PrOH:Me₂CO (v/v)] to give the desired product (0.53 g, 19%) as a pale yellow oil: ¹H NMR (CDCl₃) 1.245 (br s, 36 H, -CH₂-), 1.46 (m, 8 H, NCH₂CH₂-(CH₂)₁₀), 2.5 (m, 8 H, NCH₂(CH₂)₁₁), 2.8 (m, 32 H, NCH₂CH₂O, NCH₂CH₂Ind), 3.6 (m, 48 H, NCH₂CH₂), 7.1 (m, 6 H, aromatic), 7.33 (d, 2 H, aromatic), 7.56 (dd, 2 H, aromatic), and 8.68 (br. s, 2 H, aromatic); ¹³C NMR 136.2, 126.7, 122.51, 121.474, 118.85, 118.55, 114.0, 111.103, 70.68, 69.85, 56.30, 56.14, 55.93, 54.20, 54.03, 53.84, 29.59, 27.48, 26.86, 23.02, and 27.09; HRMS [FAB, (M + H)⁺] calcd for C₈₀H₁₄₁N₈O₁₂ 1406.06707, found 1406.06100.

N,N'-Bis{12-[N-(N'-2-(1-methylindolyl)ethyl)diaza-18-crown-6]-dodecyl}diaza-18-crown-6, Me-InCH₂CH₂(N18N)(CH₂)₁₂(N18N)(CH₂)₁₂(N18N)CH₂CH₂In-Me, 2. (a) *N*-Methyl-3-(2-bromoethyl)-indole. NaH (in oil, 1.8 g) and CH₃I (14.2 g, 100 mmol) were mixed in dry THF (15 mL). A solution of 3-(2-bromoethyl)indole (2.24 g, 10.0 mmol) in THF (50 mL) was added during 30 min at 25 °C, the mixture was stirred for 48 h, filtered, concentrated in vacuo, and dissolved in CHCl₃, and the organic phase was washed with H₂O (3 × 50 mL). The organic phase was dried over MgSO₄ and filtered, and silica gel (2 g) was added. The resulting slurry was shaken (15 s) and filtered. The organic phase was concentrated in vacuo to give a clear oil (2.17 g, 91%). The ¹H NMR spectrum was in accord with the values reported in the literature.⁴⁴

(b) *N*-(*N*-Methyl-3-ethyl)indolyl)-4,13-diaza-18-crown-6. A solution of diaza-18-crown-6 (2.62 g, 10.0 mmol), *N*-methyl-3-(2-bromoethyl)indole (2.14 g, 9.0 mmol), Na₂CO₃ (10.60 g, 100 mmol), and KI (0.17 g) in butyronitrile (200 mL) was heated (reflux, round-bottomed flask) for 24 h. The mixture was filtered and concentrated in vacuo, and the dark yellow oil was purified by flash column chromatography (silica, Me₂CO, and Me₂CO/Et₃N (9:1) and 50% CH₂Cl₂/Me₂CO, Me₂CO, and 10% Et₃N/Me₂CO) to give two fractions. Fraction 1 contained Me-InCH₂CH₂(N18N)CH₂CH₂In-Me and some alkylating agent (TLC). Fraction 2 contained Me-InCH₂CH₂(N18N)H (1.22 g, 32%) which was a light yellow oil that darkened on standing. ¹H NMR (CDCl₃): 2.80 (m, In-CH₂CH₂-N, 4H), 2.919 (m, N-CH₂CH₂O, 8H), 3.62 (m, N-CH₂CH₂O, 16H), 3.73 (s, N-CH₃, 3H), 6.88 (s, 1H, indole), 7.09 (t, 1H, indole), 7.26 (m, 2H, indole), 7.58 (d, 1H, indole).

N,N'-Bis{12-[N-(N'-2-(1-methylindolyl)ethyl)diaza-18-crown-6]-dodecyl}diaza-18-crown-6. A solution of the monosubstituted crown (0.73 g, 1.74 mmol), *N,N'*-bis(12-bromododecyl)diaza-18-crown-6 (BrC₁₂(N18N)C₁₂Br) (0.643 g, 0.87 mmol), Na₂CO₃ (0.53 g, 5.0 mmol), KI (0.017 g, 0.1 mmol), and butyronitrile (3.0 mL) was heated to reflux temperature in a round-bottomed flask for 48 h. The reaction mixture was filtered and the solvent removed in vacuo. The dark yellow oil was suspended in 50 mL of toluene and concentrated in vacuo again. The oil obtained was dissolved in 100 mL of ethyl acetate. The organic layer was washed with water (3 × 25 mL), dried (MgSO₄), and filtered, and the solvent was removed in vacuo. The resulting oil was purified by flash column chromatography (silica, Et₃N/Me₂CO, 0–5%) to afford a yellow oil that solidified upon standing. This solid was suspended in 30 mL of hot diethyl ether, and CH₂Cl₂ was added dropwise until a clear solution was obtained. The solution was cooled in a freezer and filtered, and the residue was washed with cold ether. *N*-Methylindole channel was obtained as an off-white solid (0.33 g, 36% yield): mp 75–77 °C; ¹H NMR (CDCl₃) 1.23 (m, -CH₂-, 32 H), 1.41 (m, NCH₂CH₂, 8H), 2.46 (m, NCH₂CH₂, 8H), 2.76 (m, In-CH₂CH₂-N and InCH₂CH₂-N-CH₂CH₂O, 16H), 2.89 (m, N-CH₂CH₂O, 16H), 3.62 (m, N-CH₂CH₂O, 48H), 3.72 (s, N-CH₃, 6H), 6.85 (s, indole, 2H), 7.07 (t, indole, 2H), 7.19–7.24 (m, indole, 4H), 7.55 (d, indole, 2H); IR

(KCl) 2923, 1463 1352, 1124 cm⁻¹. Anal. Calcd for C₈₂H₁₄₄N₈O₁₂: C, 68.68; H, 10.12; N, 7.81. Found: C, 68.80; H, 10.06; N, 7.84.

N,N'-Bis(N-(N'-(dansyldiaza-18-crown-6)dodecyl)diaza-18-crown-6, N(N18N)C₁₂(N18N)C₁₂(N18N)Dn, 3. Compound 6 (qv, 0.39 g, 0.35 mmol) was dissolved in 10 mL of CH₂Cl₂ and 0.5 mL of Et₃N, and the solution was placed in a water/ice bath. After half an hour a solution of dansyl chloride (0.229 g, 0.85 mmol) in 5 mL of CH₂Cl₂ was added dropwise. After 48 h the reaction was stopped and concentrated in vacuo. The resulting yellow solid was purified by column chromatography (alumina, 0–5% MeOH/CHCl₃) to give a green oil (0.45 g, 81% yield): ¹H NMR (CDCl₃) 1.20 (m, -CH₂-, 32 H), 1.38 (m, NCH₂CH₂, 8H), 2.43 (m, NCH₂CH₂, 8H), 2.72 (m, CH₂NCH₂CH₂O, 16H), 2.82 (s, NCH₃, 12H) 3.62 (m, S-NCH₂CH₂O and NCH₂CH₂O, 56H), 7.12 (d, dansyl, 2H), 7.49 (m, dansyl, 4H), 8.11 (d, dansyl, 2H), 8.26 (d, dansyl, 2H), 8.46 (d, dansyl, 2H); IR (KCl) 3418, 2927, 1572 1111, 1077 cm⁻¹; high-resolution FAB mass spectra for C₈₄H₁₄₄N₈O₁₆S₂ calcd 1586.0219 g/mol, found 1586.0242 g/mol.

N,N'-Bis(12-bromododecyl)diaza-18-crown-6, A, was prepared as previously reported.⁸

N,N'-Didansyl-4,13-diaza-18-crown-6, 4, was prepared as reported.²⁰

N,N'-Bis{12-[N-(N'-dodecyl)diaza-18-crown-6]dodecyl}diaza-18-crown-6, C₁₂H₂₅(N18N)(CH₂)₁₂(N18N)(CH₂)₁₂(N18N)C₁₂H₂₅, 5, was prepared as previously reported.⁸

N,N'-Bis{N-[12-(N-benzyl)diaza-18-crown-6]dodecyl}diaza-18-crown-6, 6, was prepared as previously reported.⁸

Monte Carlo Simulations. The fragments modeled were drawn using MacroModel and minimized to convergence using the truncated Newton method.⁴⁵ The parameters used were from the all-atom AMBER force field, and the solvent treatment was the GB/SA CHCl₃ or water solvation models. The minimized structure was consequently used as the starting point for the Monte Carlo multiple minimum search. This command causes an input structure to be modified by random changes in its torsion angles.⁴⁶ The alkyl chain was constrained in an all-gauche conformation. The search was continued until a global minimum was found at least five times. The resulting family of structures was minimized. Only structures that were within a 3-kcal window from the global minimum were taken into account.

FT-IR Analysis of Indole Channel 1. A series of solutions of indole channel 1 in CCl₄ were prepared. The channel concentrations ranged from 10⁻² to 10⁻⁴ M. The samples were placed in IR-grade cuvettes. The IR spectrum was taken for every solution, covering a spectral window from 4000 to 400 cm⁻¹.

Steady-State Fluorescence of Indolyl (1), N-Methylindolyl (2), and Dansyl (3) Channels. (a) **Vesicle Preparation.** A solution of phosphatidylglycerol (1.30 mL, 10 mg/mL in CHCl₃) and a solution of phosphatidylcholine (0.52 mL, 100 mg/mL in CHCl₃/MeOH (98:2)) were placed in a 15 mL test tube. The CHCl₃ was removed in vacuo and the system left overnight under high vacuum. The resulting film was suspended in buffered saline solution (1:10 dilution, 10 mL). The suspension was then sonicated with a Branson tip sonicator (duty cycle 50%, setting 4, 20 min) in an ice bath. The resulting translucent suspension was filtered through a 0.2 μm polycarbonate membrane filter. Particle sizes of ~750 Å were obtained as determined by laser light scattering.

(b) **Ionophore Incorporation.** To 1.0 mL of vesicle suspension were added 30 μL of a 10⁻⁴ M solution of the corresponding fluorescent ionophore. The vesicles were incubated at 60 °C for 1 h in a water bath. The vesicle suspension was then diluted to 3.0 mL with doubly distilled water, and the fluorescence emission spectrum of the sample was obtained.

(c) **Fluorescence Spectra of Channels in Solution.** A 10⁻³ M solution of the corresponding fluorescent ionophore was made in MeOH. From this solution 10.0 μL aliquots were taken and placed in 10.0 mL volumetric flasks. The samples were diluted to the mark with the corresponding solvent to obtain 10⁻⁶ M solutions of the fluorescent channels. The fluorescence emission spectrum was obtained as before.

(44) Rahman, A.-U.; Sultana, M.; Hassan, I.; Hassan, N. *J. Chem. Soc., Perkin Trans. 1* 1983, 2093.

(45) Ponder, J. W.; Richards, F. M. *J. Comput. Chem.* 1987, 8, 1016.
(46) Chang, G.; Guida, W. C.; Still, W. C. *J. Am. Chem. Soc.* 1989, 111, 4379.

Depth Dependent Quenching of Dansyl Channel (3) Fluorescence in Phospholipid Bilayers. Vesicle Preparation. Solutions of the phosphatidylcholine distearoyl and either 1-palmitoyl-2-stearoyl-(12-doxyl)-*sn*-glycero-3-phosphocholine or 1-palmitoyl-2-stearoyl-(7-doxyl)-*sn*-glycero-3-phosphocholine (2.28×10^{-3} M) were prepared in CH_2Cl_2 . Varying volumes of the phosphatidylcholine solution (0 to 125 mL) were placed in Eppendorf vials, and doxyl phospholipid solution was added to a total volume of 125 mL. The mole fraction of the doxyl phospholipid was therefore varied from zero to one, while keeping the total concentration of lipids constant. The solvent was then removed from all vials with a nitrogen stream. The vials were set under high vacuum overnight. To each vial was then added a 1.0 mL solution of the saline (1:10) buffer, and each sample was sonicated for 2 min using a tip sonicator (setting 2, duty cycle 50%). The samples were kept under nitrogen and in an ice/water bath. To each vial was then added 30 μL of a 1×10^{-4} M solution of dansyl channel in $\text{CF}_3\text{CH}_2\text{OH}$ ([lipid]:[channel] = 1:100). These solutions were incubated at 60 °C for 1 h. Each solution was diluted to 3.0 mL using the saline buffer (1:10). The final channel concentration in each sample was 1×10^{-6} M. Fluorescence emission spectra were taken for each sample. The distance of the fluorescent probe from the center of the bilayer was calculated by determining the ratio of the fluorescence intensity of each sample and the fluorescence intensity of the sample in the absence of doxyl lipid. The natural logarithm of these numbers was plotted against the mole fraction of doxyl lipid in each sample. The two sets of data obtained from two 7- and 12-doxyl labeled lipids were fitted to the equations previously discussed using least-squares fitting with Scientist⁴⁷ software package.

(47) Scientist for Windows, version 2.01 was obtained from MicroMath Scientific Software, Salt Lake City, UT 84121.

Fluorescence Energy Transfer Experiment between *N*-Methylindole and Dansyl Channel in Phospholipid Bilayers. (a) Vesicle Preparation. Phospholipid vesicles were prepared as above.

(b) Insertion of Ionophore. Solutions of the dansyl (3) and methylindole (2) channels (1×10^{-3} M) were prepared in $\text{CF}_3\text{CH}_2\text{OH}$. To 1.0-mL samples of the vesicle suspension were added aliquots of these channel compound solutions, varying in volume from 0 to 30 μL . The mole fraction of the dansyl channel was thus varied from zero to one, while keeping the total concentration of ionophore constant. These solutions were placed in Eppendorf vials and were incubated at 60 °C for 1 h. Each solution was made up to 3.0 mL using saline (1:10) buffer solution. The final concentration of channel in each sample was thus 1×10^{-5} M.

(c) Fluorescence Measurements. Three sets of fluorescence measurements were performed. First, each sample was irradiated at 283 nm. Every sample that included methylindole channel 2 exhibited a typical emission profile with a maximum wavelength at 340 nm. Second, each sample was irradiated at 340 nm. The samples that contained the dansyl channel (3) compound displayed a similar result, giving emission profiles with the maximum wavelength at 520 nm. Third, the samples were irradiated at 283 nm and their fluorescence emission spectra were recorded between 460 and 560 nm. No peak at 520 nm was observed over the range of samples in these experiments although a very weak and broad band was detected at $\lambda_{\text{max}} = 513$ nm in all cases in which 2 was present. In addition, in all cases in which phospholipid vesicles were present, a sharp diffraction band was observed at $\lambda_{\text{max}} = 565$ nm.

Acknowledgment. We thank the NIH for Grant GM-36262 that supported this work.

JA9909172